

Supporting information

Use of Comparative Molecular Field Analysis, Comparative Molecular Similarity Indices Analysis, and Protein Homology Modeling to Elucidate the Catalytic Selectivity of Human UDP-glucuronosyltransferase 1A9"

Baojian Wu, Xiaoqiang Wang, Shuxing Zhang, Ming Hu

Table S1 Summary of the site(s) of glucuronidation for the phenolic compounds with multiple hydroxyl groups in this paper determined based on the literature.

No.	Name	Sites of Glucuronidation	References
1	EGCG	3'-OH and 4''-OH	Lu et al., 2003
2	EGC	3'-OH	Lu et al., 2003
18	Emodin	3-OH	Liu et al., 2010
20	Enterolactone	3-OH	Dean et al., 2004
22	Raloxifene	6-OH	Change et al., 2009
26	Hesperetin	3'-OH and 7-OH	Brand et al., 2010
27	Narigenin	7-OH	Xu et al., 2009
55	Flavopiridol	7-OH	Ramírez et al., 2002
97	Caffeic acid	3-OH and 4-OH	Wong et al., 2010
100	Biochanin A	7-OH	Chen et al., 2005
101	Daidzein	7-OH	Zhang et al., 1999
102	Dihydrodaidzein	7-OH*	Wu et al., 2011
103	Equol	7-OH*	Wu et al., 2011
104	Formononetin	7-OH	Chen et al., 2005
105	Genistein	7-OH	Zhang et al., 1999
106	Glycitein	7-OH	Chen et al., 2005
108	Prunetin	5-OH	Joseph et al., 2007
138	Resveratrol	3-OH	Brill et al., 2006
140	Entacapone	3-OH	Lautala et al., 2000
142	Mycophenolic acid	4-OH	Change et al., 2009
145	Tolcapone	3-OH	Lautala et al., 2000

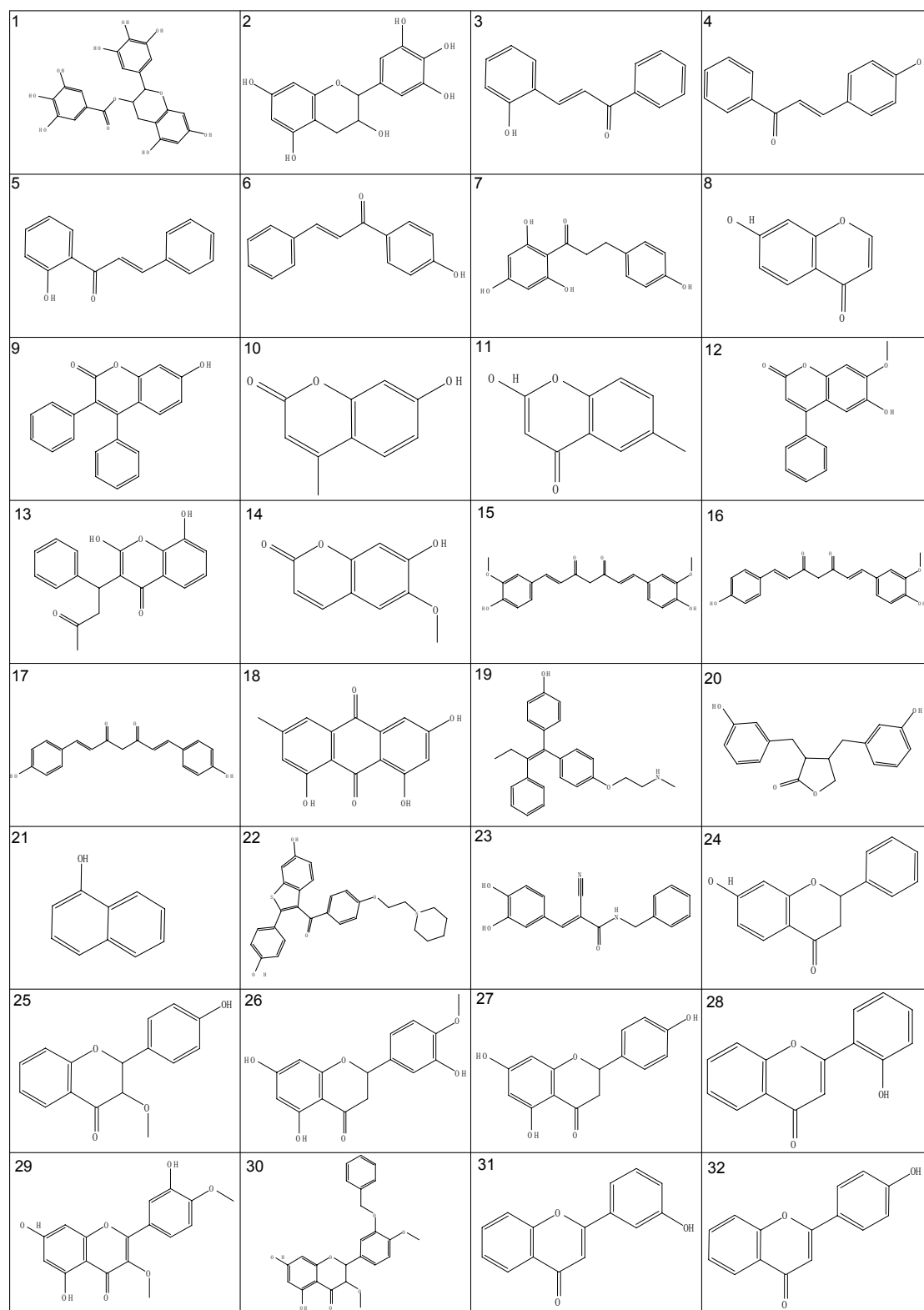
* Based on the fact that 7-OH group in the isoflavone backbone is the most favorable position for glucuronidation.

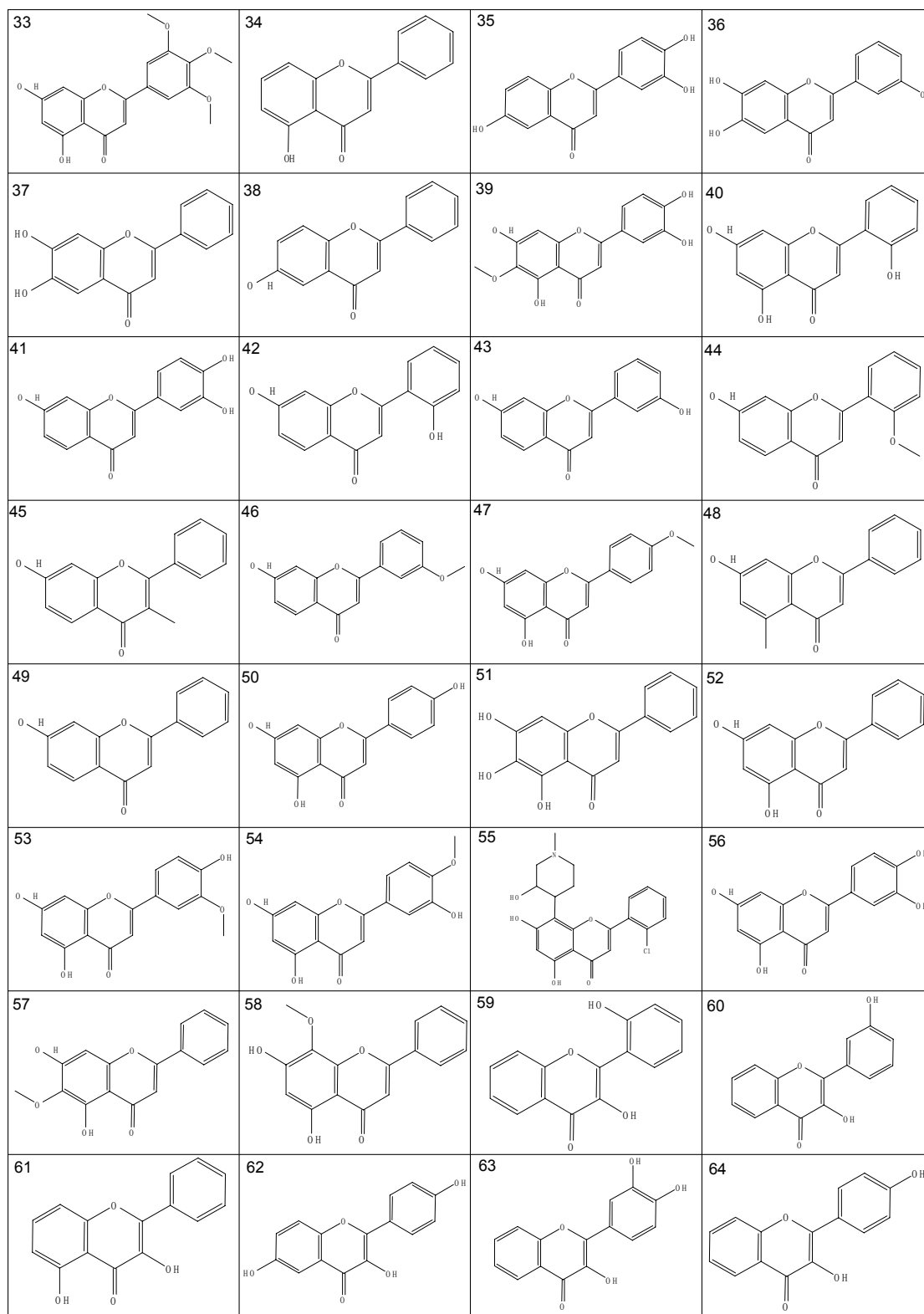
Brand W, Boersma MG, Bik H, Hoek-van den Hil EF, Vervoort J, Barron D, Meini W, Glatt H, Williamson G, van Bladeren PJ, Rietjens IM (2010) Phase II metabolism of hesperetin by individual UDP-glucuronosyltransferases and sulfotransferases and rat and human tissue samples. *Drug Metab Dispos.* **38**(4):617-25.

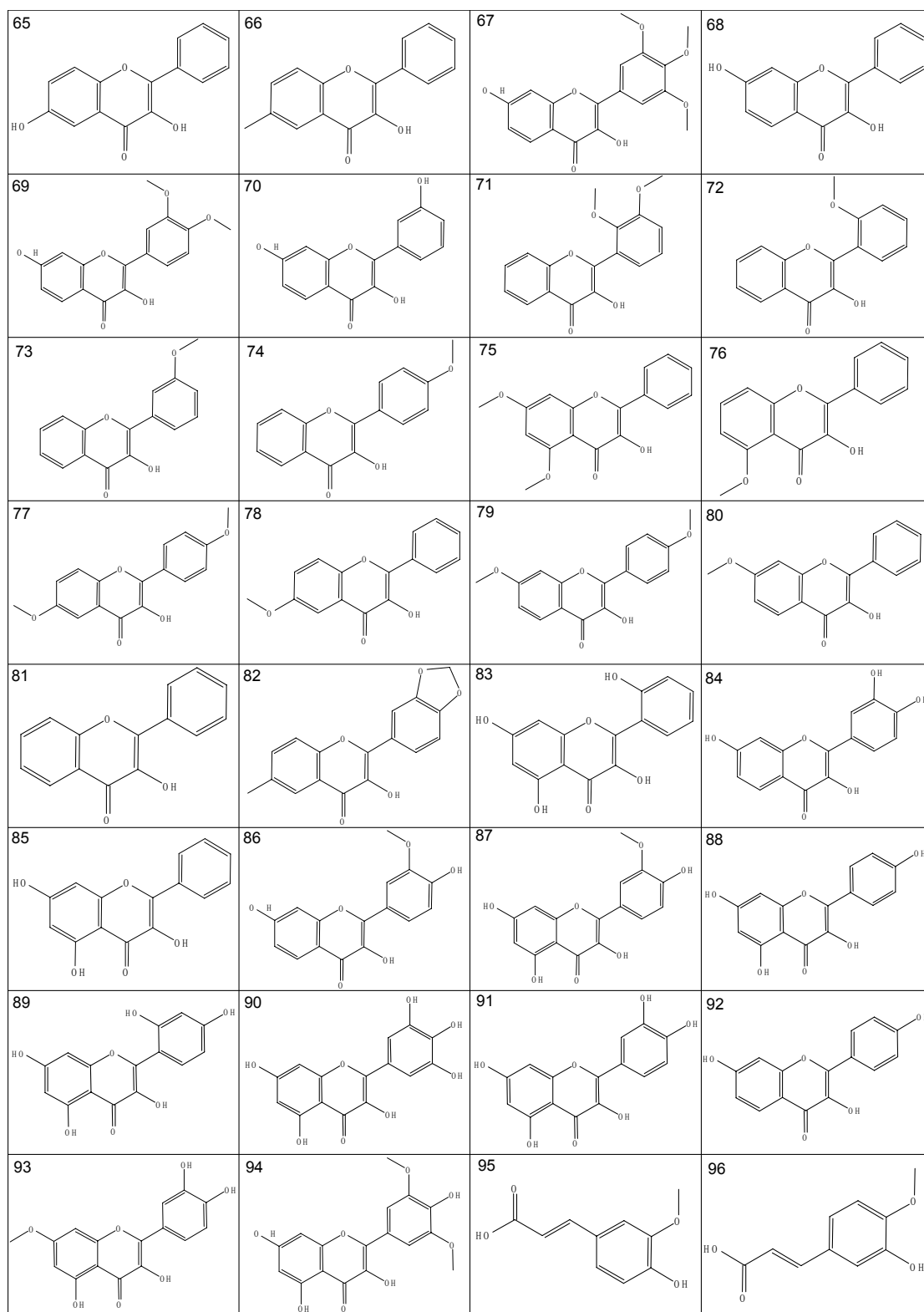
Brill SS, Furimsky AM, Ho MN, Furniss MJ, Li Y, Green AG, Bradford WW, Green CE, Kapetanovic IM, Iyer LV (2006) Glucuronidation of trans-resveratrol by human liver and intestinal microsomes and UGT isoforms. *J Pharm Pharmacol.* **58**(4):469-79.

- Chang JH, Yoo P, Lee T, Klopff W, Takao D (2009) The role of pH in the glucuronidation of raloxifene, mycophenolic acid and ezetimibe. *Mol Pharm.* **6**(4):1216-27.
- Chen J, Lin H, Hu M (2005) Absorption and metabolism of genistein and its five isoflavone analogs in the human intestinal Caco-2 model. *Cancer Chemother Pharmacol.* **55**(2):159-69.
- Dean B, Chang S, Doss GA, King C, Thomas PE (2004) Glucuronidation, oxidative metabolism, and bioactivation of enterolactone in rhesus monkeys. *Arch Biochem Biophys.* **429**(2):244-51.
- Joseph TB, Wang SW, Liu X, Kulkarni KH, Wang J, Xu H, Hu M (2007) Disposition of flavonoids via enteric recycling: enzyme stability affects characterization of prunetin glucuronidation across species, organs, and UGT isoforms. *Mol Pharm.* **4**(6):883-94.
- Lautala P, Ethell BT, Taskinen J, Burchell B (2000) The specificity of glucuronidation of entacapone and tolcapone by recombinant human UDP-glucuronosyltransferases. *Drug Metab Dispos.* **28**(11):1385-9.
- Liu W, Tang L, Ye L, Cai Z, Xia B, Zhang J, Hu M, Liu Z (2010) Species and gender differences affect the metabolism of emodin via glucuronidation. *AAPS J.* **12**(3):424-36.
- Lu H, Meng X, Li C, Sang S, Patten C, Sheng S, Hong J, Bai N, Winnik B, Ho CT, Yang CS. Glucuronides of tea catechins: enzymology of biosynthesis and biological activities (2003) *Drug Metab Dispos.* **31**(4):452-61.
- Ramírez J, Iyer L, Journault K, Bélanger P, Innocenti F, Ratain MJ, Guillemette C (2002) In vitro characterization of hepatic flavopiridol metabolism using human liver microsomes and recombinant UGT enzymes. *Pharm Res.* **19**(5):588-94.
- Wong CC, Meini W, Glatt HR, Barron D, Stalmach A, Steiling H, Crozier A, Williamson G (2010) In vitro and in vivo conjugation of dietary hydroxycinnamic acids by UDP-glucuronosyltransferases and sulfotransferases in humans. *J Nutr Biochem.* **21**(11):1060-8.
- Wu B, Kulkarni K, Basu S, Zhang S, Hu M (2011) First-pass metabolism via UDP-glucuronosyltransferase: a barrier to oral bioavailability of phenolics. *J Pharm Sci.* **100**(9):3655-81.
- Xu H, Kulkarni KH, Singh R, Yang Z, Wang SW, Tam VH, Hu M (2009) Disposition of naringenin via glucuronidation pathway is affected by compensating efflux transporters of hydrophilic glucuronides. *Mol Pharm.* **6**(6):1703-15.
- Zhang Y, Song TT, Cunnick JE, Murphy PA, Hendrich S (1999) Daidzein and genistein glucuronides in vitro are weakly estrogenic and activate human natural killer cells at nutritionally relevant concentrations. *J Nutr.* **129**(2):399-405.

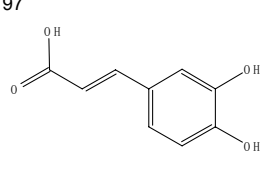
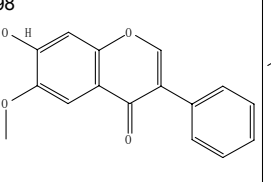
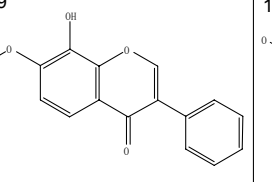
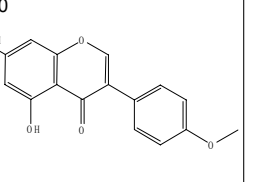
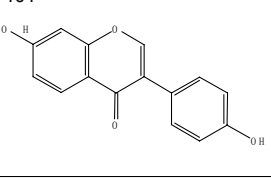
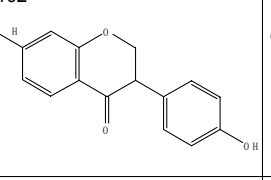
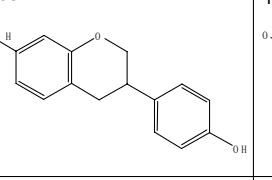
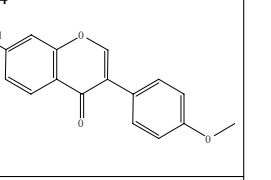
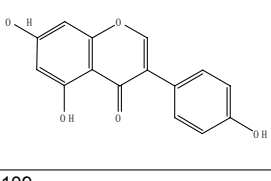
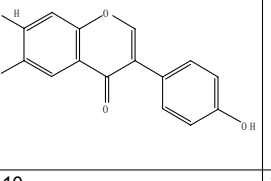
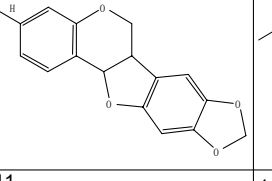
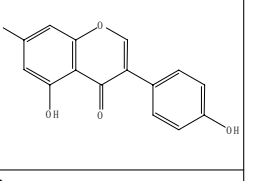
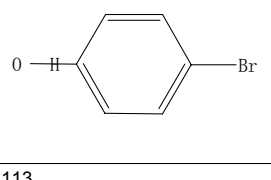
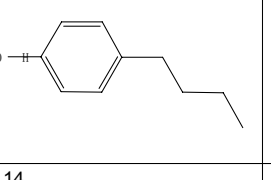
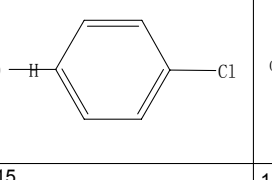
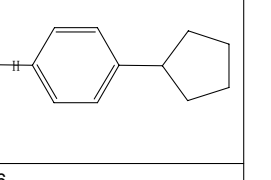
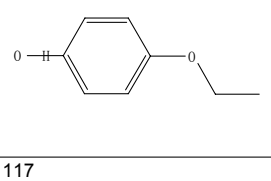
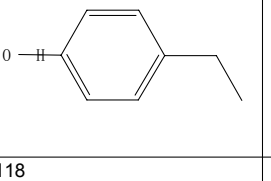
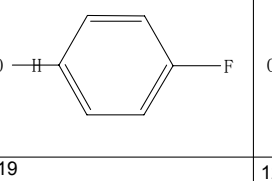
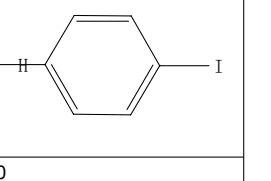
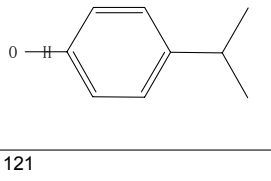
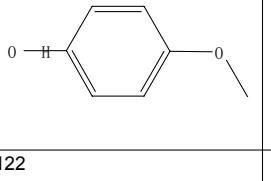
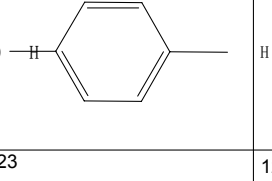
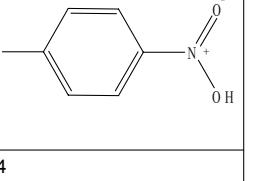
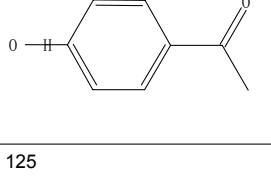
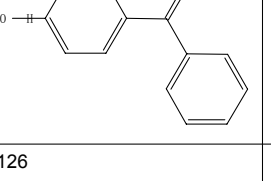
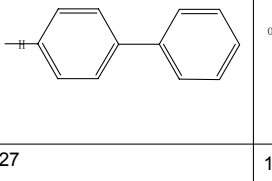
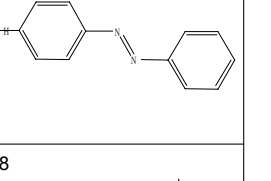
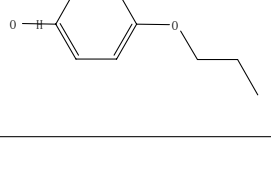
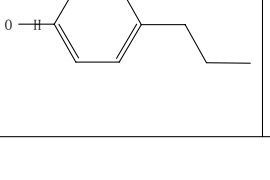
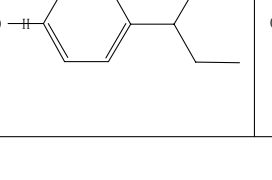
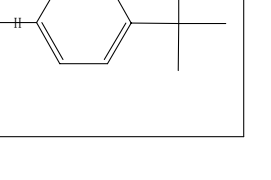
Figure S1 Chemical structures of 145 UGT1A9 substrates in this study. Numbering of the structures is consistent with that in Table 1.







Journal of Medicinal Chemistry

<p>97</p> 	<p>98</p> 	<p>99</p> 	<p>100</p> 
<p>101</p> 	<p>102</p> 	<p>103</p> 	<p>104</p> 
<p>105</p> 	<p>106</p> 	<p>107</p> 	<p>108</p> 
<p>109</p> 	<p>110</p> 	<p>111</p> 	<p>112</p> 
<p>113</p> 	<p>114</p> 	<p>115</p> 	<p>116</p> 
<p>117</p> 	<p>118</p> 	<p>119</p> 	<p>120</p> 
<p>121</p> 	<p>122</p> 	<p>123</p> 	<p>124</p> 
<p>125</p> 	<p>126</p> 	<p>127</p> 	<p>128</p> 

Journal of Medicinal Chemistry

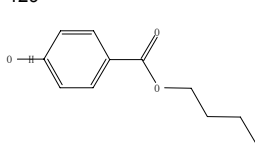
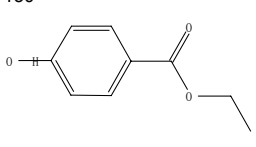
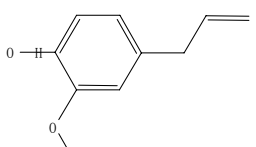
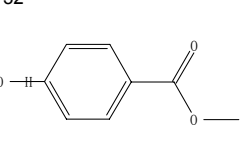
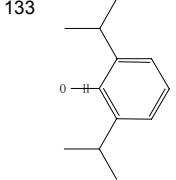
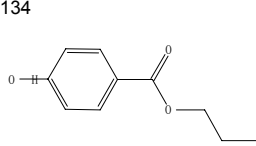
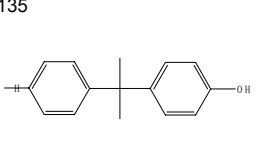
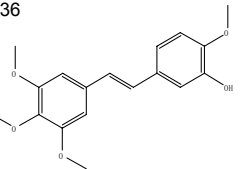
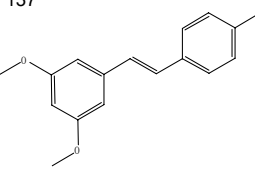
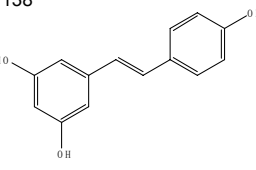
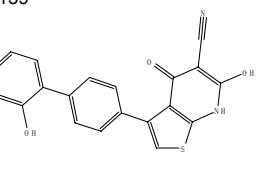
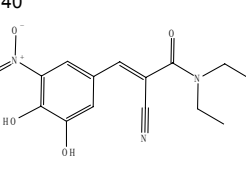
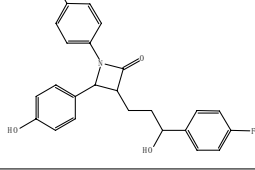
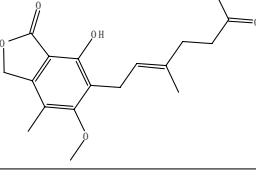
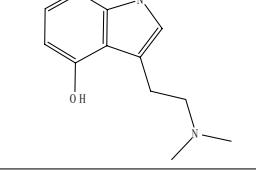
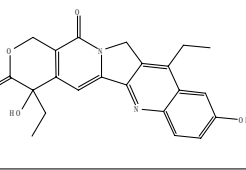
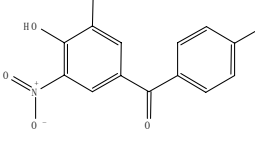
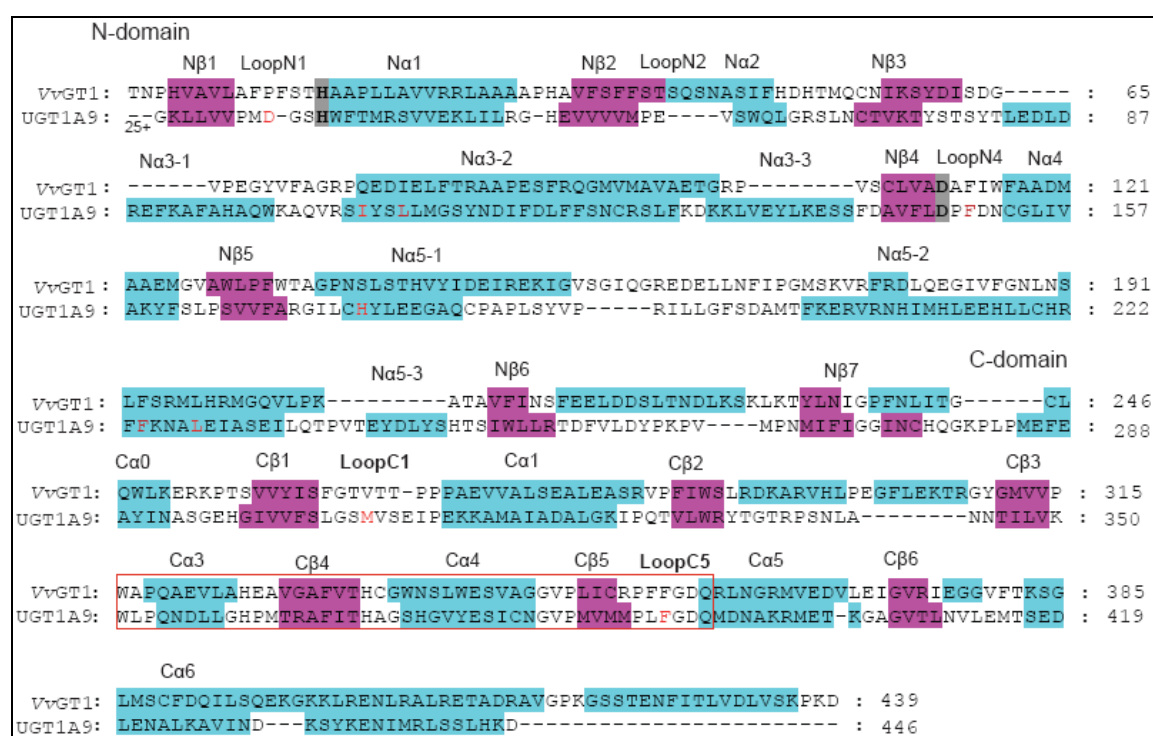
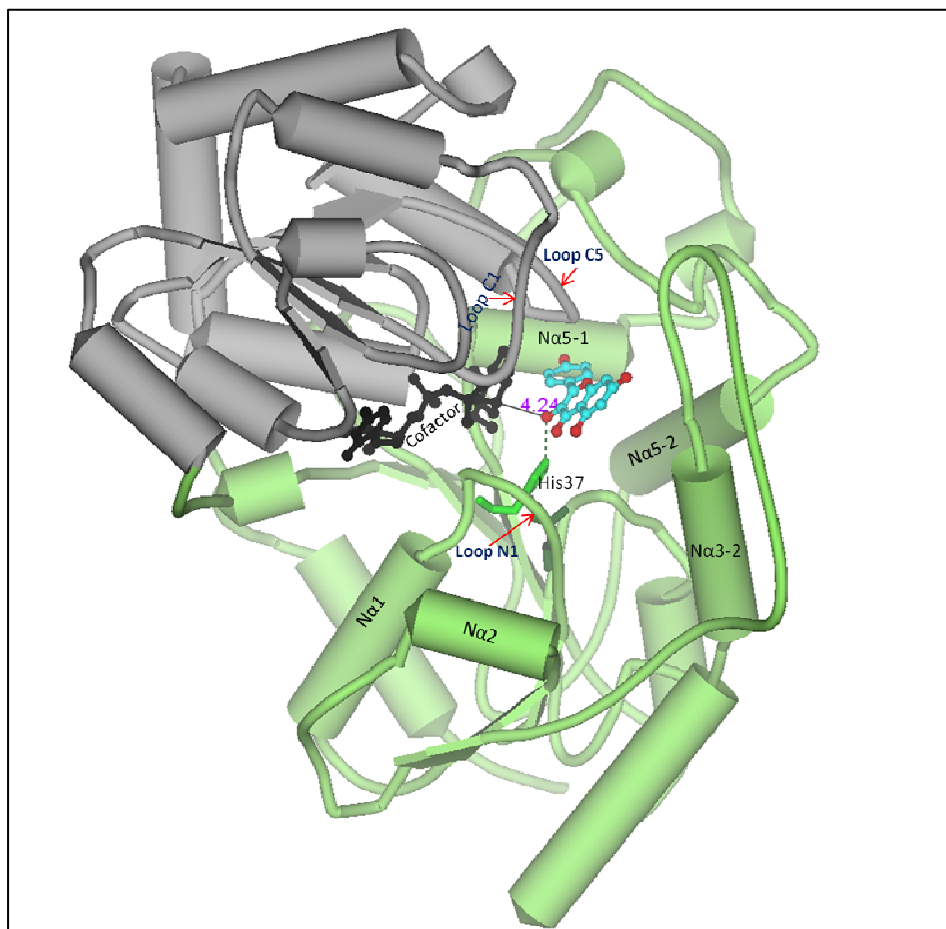
<p>129</p> 	<p>130</p> 	<p>131</p> 	<p>132</p> 
<p>133</p> 	<p>134</p> 	<p>135</p> 	<p>136</p> 
<p>137</p> 	<p>138</p> 	<p>139</p> 	<p>140</p> 
<p>141</p> 	<p>142</p> 	<p>143</p> 	<p>144</p> 
<p>145</p> 			

Figure S2 Protein sequence alignment of human UGT1A9 with the plant VvGT1 (pdb code: 2C1Z). The aligned sequence identity between UGT1A9 and VvGT1 is 14.9%. Secondary structures (α -helix in cyan, β -strands in magenta) are color shaded. The secondary structures of the human UGTs were determined by PSIPRED (McGuffin *et al.*, 2000). The 44-aa signature motif of UGTs is enclosed by a red box. Residues predicted to be in contact with aglycone substrate are highlighted in red, whereas the catalytic dyad residues (His37-Asp148) are highlighted in grey.



McGuffin LJ, Bryson K and Jones DT (2000) The PSIPRED protein structure prediction server. *Bioinformatics*. 16:404-405.

Figure S3 A homology model of UGT1A9 constructed in the paper and the description of the binding pocket. The modeled structures are composed of two N- (in gray) and C-terminal (in light green) domains. The N- and C-terminal domains contain central stranded parallel sheets flanked by α -helices on both sides. The two domains pack very tightly and form a deep cleft where the aglycone substrate and the cofactor are bound for reaction. N α 5-2 packs to N α 3-2, facilitating specific interactions (e.g. salt bridge) between the two regions. These interactions might play a role in the entry of the aglycone and in the departure of the product (Modolo *et al.*, 2009; Laakkonen and Finel, 2010). It was also proposed that residues in N α 3-2 area might go through some local conformational changes during substrate binding and subsequent product leaving (Modolo *et al.*, 2009). The substrate binding pocket is almost entirely formed by the N-terminal residues, although some C-terminal residues also contributed to the formation of the pocket. The pocket is primarily formed by LoopN1, N α 1, N α 3-2, LoopN4, N α 5-1, N α 5-2, Loop C1 and Loop C5. This is consistent with the topological arrangement of β -strands (3-2-1-4-5-6-7) of the UGT enzyme. N β 2, N β 3, N β 6 and N β 7 twisted far away from the core N β 1 where the catalytic histidine situated. Loop N4 was located at the bottom of the pocket (far from the cofactor); N α 5-1 residues formed the wall in the end of the pocket; Loop N1 and N α 3-2 line the entrance of the pocket; Loop C1 and C5 cover the top of the pocket; the right side of the pocket is occupied by the residues in the N-terminus of N α 5-2. The cofactor is present at the left side of pocket. The catalytic residue histidine (in green stick mode) was located at the start of helix N α 1. The substrate kaempferol (in a 3-OH catalysis mode) is shown in stick-and-ball model.



Journal of Medicinal Chemistry

- Laakkonen L and Finel M (2010) A molecular model of the human UGT1A1, its membrane orientation and the interactions between different parts of the enzyme. *Mol Pharmacol* **77**(6):931-939
- Modolo LV, Li L, Pan H, Blount JW, Dixon RA, Wang X (2009) Crystal structures of glycosyltransferase UGT78G1 reveal the molecular basis for glycosylation and deglycosylation of (iso)flavonoids. *J Mol Biol.* **392**(5):1292-302.